Geometric Dimensional Measurement of Shearer Rotational Parts

Chenxu Luo
China University of Mining and Technology, Xuzhou, China
Email: xzhlunwen@163.com

Changlong Du* and Wan Ma
China University of Mining and Technology, Xuzhou, China
Email: xzhqingting@163.com, mawan333@163.com

***Abstract*—A geometric dimensional measurement system for form and position error detection of shearer rotational parts is developed in this paper with the error evaluation principle based on the minimum zone method. The system is characterized by using the charge coupled device (CCD) image sensor to capture image signals, and then using image processing techniques to extract useful signals from the image data signal. By focusing on image processing technology and error separation technology, the system can reduce the previous dependence on the baseline data collection, improve the accuracy and robustness of data collection, and simplify data collection platform.**

***Index Terms*—shearer rotational parts, geometric dimensional measurement, CCD image sensor, error separation**

I. Introduction

Normally, the shearer assembly process gets into trouble as some axes of the traction unit and cutting unit are out of alignment, which is due to the low geometric precision of parts; in the coal mining operation, the failure of geometric precision will perform great damage to the transmission unit. Great inconvenience will be brought to the manufacture of shearers in these circumstances, and large economic losses will be made. This shows the importance of doing research on geometry tests of rotary parts [1-3].

With the development of computer monitoring and control technology, the dimensional measurement of large-size rotary parts begins to be aimed at fast, accurate and reliable visual inspection around the world. These technologies are involved in optics, electronics and computer integrated technologies. Foreign researchers brought visual inspection into a coordinate measuring machine, by analyzing the change of CMM probe position in the visual system to determine the spatial coordinates of measured points; some scholars applied to the visual detection into the detection of non-mechanical parts received good results [4-6]. Scholars in China have done a great visual inspection-related research, and applied the visual inspection into the detection of mechanical parts [7-10]. The study shows that scientists and researchers focus on accurate visual detection [11-13]. However, most studies related to signal processing of image processing is not deep enough, and large rotary part of the vision measurement by the CCD image sensor size restrictions, are not widely used [14-16].

In this paper, geometrical detection of shearer rotary parts is carried out based on the use of CCD image sensor and Gauss Laplace image processing program.

II. CCD Image Data Acquisition

A. Parallel Light Projection Method

The measurement device (shown in Fig. 1) measures the object size using the parallel light projection method. The lighting system produces parallel light and the profile of the object is projected on the CCD, so that size changes are truly reflected in the line array CCD. And then the size of the object is obtained.

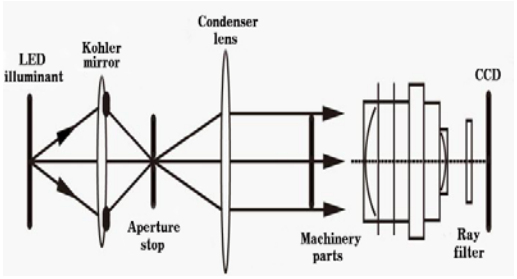

Figure 1. Schematic of a CCD measuring device.

To achieve better detection of rotary part geometry the method of backlight illumination is used. It indicates that light source and CCD are located on different sides. A backlight source produces an intensively contrastive contour of the measured object, which can be used to detect the contour size. The infrared lighting with a longer wavelength and better illumination uniformity is selected for profile measurement. The lighting installation use the form of Kohler illumination and the color of the LED light source is red.

B. Parallel Light Projection Method

As for large-size, high precision automatic measurement of outer diameter of coal mining machinery rotary parts, the measurement accuracy

doi:10.4304/jcp.8.12.3204-3209

and the measurement range are limited due to the CCD pixel size and the pixel number. It is necessary to splice two and even multi-chip CCD together, to use the CCD in the measurement instrument.

Under the measuring microscope, a four-dimensional adjusting mechanism is needed to achieve splicing the sensitive elements of two linear array CCD on the uniform stitching line in the same plane within a certain tolerance. The error Δ y, produced by the two linear array CCD being not coplanar, would cause the image clarity error and the horizontal magnification of the sensitivity image receiver of the two linear array CCD; projection errors would be caused due to two declination angles of the two linear array CCD in two different directions. The error Δ x would produce the inconsistency of diameter measurement. So, those errors are all needed to be adjusted. The formula for diameter calculation is

$$d = \frac{L_0 N_2}{\beta_1} + \frac{L_0 N_2}{\beta_2} = \frac{L_0 N_2 \beta_2 + L_0 N_2 \beta_1}{\beta_1 \beta_2}. \quad (1)$$

The d is the measured diameter; L_0 is the center distance of CCD image sensitive elements; N_1 and N_2 refer to the number of image sensitive cells obscured by the object images on the two CCD, respectively; β_1 and β_2 stand for the optical imaging lens' horizontal magnifications of the two CCD, respectively.

III. Image Processing Principles

The image processing is mainly achieved by Gaussian filter combined with Susan edge detection.

A. Gauss - Laplace Filter

Because of the presence of image noises, it is necessary to use a Gaussian low-pass filter to pre-smooth data. According to the combination law of convolution, it can be seen that the Laplacian and a Gaussian impulse response can be combined into a Gauss-Laplace nuclear, represented by

$$-\nabla^2 \frac{1}{2\pi\sigma^2} e^{-\frac{x^2+y^2}{2\sigma^2}} = \frac{1}{\pi\sigma^4}[1-\frac{x^2+y^2}{2\sigma^2}]e^{-\frac{x^2+y^2}{2\sigma^2}}. \quad (2)$$

Dates of manuscript submission, revision and acceptance should be included in the first page footnote. Remove the first page footnote if you don't have any information there. This impulse response is separable for x and y, so it can be achieved effectively. It has the same shape with the general band-pass filter's impulse response, which is similar with a positive peak existing in a negative concave valley. Parameter σ controls the width of the center peak, and consequently the degree of smooth.

B. Susan Edge Detection

The basic principle of edge and corner extraction algorithm is that the edge and corner points have the smallest USAN area. Therefore, we can detect image edges and corners and other features' location and direction information according to the size of the USAN area and matrix properties. The specific steps of Susan edge detection are to scan the entire image with a circular template, then compare the gray value of each pixel with the center pixel, and finally give threshold to determine whether the pixel belongs to the USAN area. The following equation is

$$c\left(\vec{r}, \vec{r_0}\right) = \begin{cases} 1 & if \mid I(\vec{r}) - I(\vec{r_0}) \mid \leq t \\ 0 & if \mid I(\vec{r}) - I(\vec{r_0}) \mid > t \end{cases}. \quad (3)$$

The $c(r,r_0)$ is the discriminant function of pixels that belong to the USAN region in template; $I(r_0)$ is the gray value of template center pixel; $I(r)$ is the gray value of any other pixel in template; t is the gray scale difference threshold. Then a point's USAN area size in the image can be expressed as

$$n\left(\vec{r_0}\right) = \sum_{\vec{r} \neq \vec{r}} c\left(\vec{r}, \vec{r_0}\right). \quad (4)$$

According to the size of the USAN area and matrix properties, image edges and corners and other features' location and direction information can be detected. After obtaining the size of USAS area corresponding to each pixel, the geometric threshold can be defined according to Equation (4) and an initial edge response to the edge can be produced base on the formula

$$R(\vec{r_0}) = \begin{cases} g - n(\vec{r_0}) & if \quad n(\vec{r_0}) < g \\ 0 & else \end{cases}. \quad (5)$$

The g is geometric threshold. The value of the initial edge response is in line with Susan principle, that is, the smaller the USAN area, the greater the response to the initial edge. So the edge points are determined.

IV. Intelligent Geometric Data Processing Algorithms

According to the minimum regional conditions, the keys to evaluate roundness and cylindrical error are searching for the scope of initial point and determining convergence criterion. Then the results obtained using the least square method are regarded as the initial searching point. The solving method of roundness error based on the smallest regional method is shown in Fig. 2.

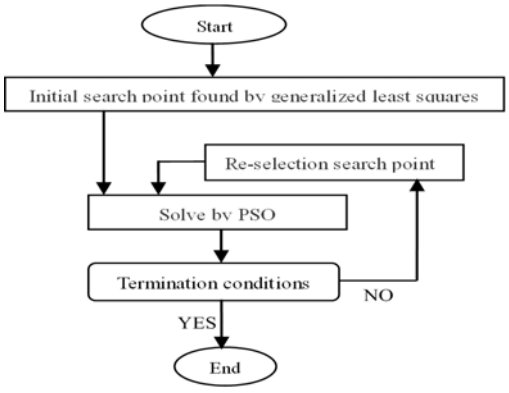

Figure 2. Schematic of a CCD measuring device.

By the fitness judgment of target, PSO will make the individuals of the group move toward to the better area on and on. The solution was looked as "particle" of the space, and its whole solution space is $X_i=(X_1,X_2,...,X_m)$, i=1, 2, …, m. d=1, 2,…, n, represent for the dimension of particles. Every particle has its fit value which is determined by target optimization function, as well as its position $x_{id}=(x_{i1},x_{i2},...,x_{in})$ and velocity $v_{id}=(v_{i1},v_{i2},...,v_{in})$ which were decided by the flight distance and direction. At first use the Algorithm take initialization on Particle, and update them through the two "extreme values", in the iteration process: one particle finds optimal value by itself, which is called "individual optimal value" as *pbest*; another finds the optimal value in the whole group, called "global optimal value" as *gbest*. After two extreme values being obtained, the velocity and position of the particle are updated and iterated constantly, until the optimal solution is found. As to form error, finding the extreme-value in a certain range is the main problem. In order to take advantage of the global exploration ability and local development ability of the particle, we use the algorithm model as follows in this article:

$$\begin{cases} v_{id}^{k+1}=\omega\times v_{id}^{k}+c_1\times rand_1^k\times(pbest^k-x_{id}^k) \\ +c_2\times rand_2^k\times(gbest^k-x_{id}^k) \\ x_{id}^{k+1}=x_{id}^k+v_{id}^{k+1} \end{cases} . \quad (6)$$

In (6), v_{id}^k is the d dimensional component of the speed of Particle i in the k iteration; c_1, c_2 are two acceleration constants, used to adjust the flight distance from particles to its *pbest* or to the *gbest*; $rand_1^k$ and $rand_2^k$ are two random numbers within [0, 1]; x_{id}^k is the d dimensional component of the position of Particle i in the k iteration; ω is the inertia weight.

The process of using PSO has two main steps in solving the optimization problem, which are the problem's encoding and fitness function's determining. Because PSO uses real-coded method, the optimized objective $o_k(x_k, y_k)$ can be regarded as a code of particle and its fitness function is defined as $f(o_k)$. Then the optimization calculation is carried out according to the PSO calculation steps. For the evaluation of roundness and cylindrical error, the following parameters are set:

Particle size *PopSize*: generally take the value from the range [20, 40], it is set to 30.

Particle dimension d: it is the search space dimension or the length of the solution; for the roundness error, $o_k(x_k, y_k)$ is regarded as a particle, so, d = 2; for the cylindrical error, $o_k(x_k, y_k, u_k, q_k)$ is regarded as a particle, so d equals to 4.

Particle range: it is generally determined according to the measurement point's distribution, the key is to determine the initial value of the problem's solution; here, the value determined by the least square method is used as the initial value.

Maximum speed *Vmax*: it is the largest moving distance of a particle in an iteration; here it is normally set as the width of the particle range.

Inertia weight ω: its initial value is 0.9 and its terminate value is 0.4 in the way of linear change.

Termination conditions: when the maximum number of iterations *MaxIteration*=100 is reached, the optimization process is terminated.

V. Experimental Results And Analysis

A. Signal Collection

A shaft, which has a basic radius value of 50 mm, of a shearer in coal is used as a measured object. According to face indexing, four axial projection plane information at 30°, 75°, 135°, 180°, shown in Figure 3, are collected.

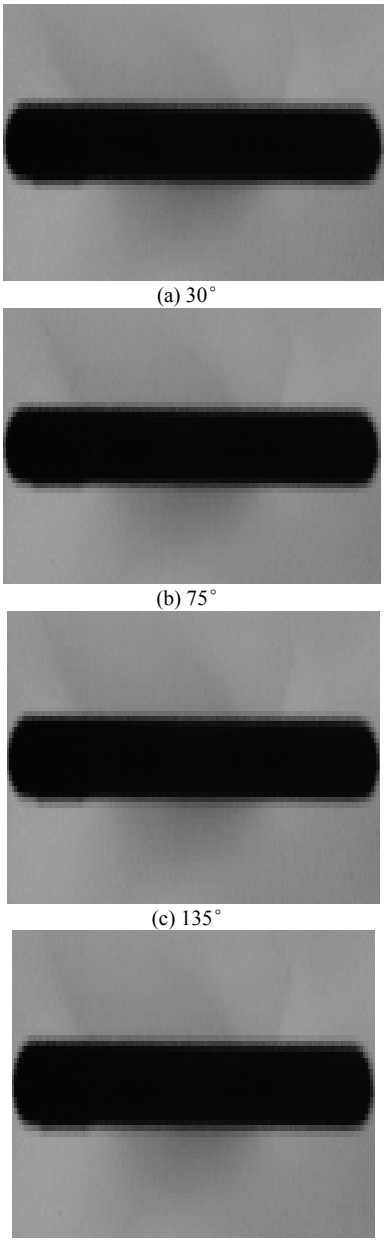

(a) 30°

(b) 75°

(c) 135°

(d) 180°

Figure 3. Four axial projection plane information

B. Image Processing

We use Gauss - Laplace filters to eliminate the four collected image signals' gross error. This would improve the accuracy of the image signals and make more realistic value. After being filtered by Gauss - Laplace filter, the standard deviation of the image data series is reduced by 7.407 %, in addition to the slight reduction of the average, which means that eliminate signals with large deviation from the average. Because of the elimination of signal error, the new average decreases by 0.2 μm, as shown in Table I.

TABLE I.
COMPARISON OF SIGNAL DATA BEFORE OR AFTER GAUSS-LAPLACE FILTERING

Item	Data before being filtered (mm)	Data after being filtered (mm)
Average	0.3935	0.3933
Standard deviation	0.0081	0.0075
Variance	6.5543e-5	5.6563e-5
Standard deviation reduction	7.407%	

In addition, it is found that if we don't use Gauss-Laplace filtering algorithm and conduct the follow-up processing, the data convergent series of different measurement objects are uncertain. The roundness error of large parts can be broken down to a certain convergence of series. And the roundness error of small parts sometimes can be broken down to a certain series, then it either converge to zero or lead to the algorithms' failure. After Gauss-Laplace filtering, data can converge in less than 20 bands. The reliability and intelligent level are thereby greatly enhanced, as shown in Figure 4.

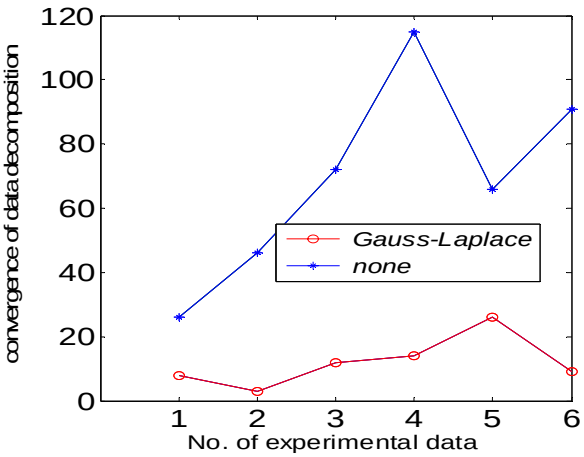

Figure 4. Four axial projection plane information.

After the gross error of the image signal is removed, gray value is used to process the filtered image. then a clearer image outline is produced and some redundant internal points are eliminated, which makes the projection plane and backlight boundary of the key components be more clearly, which facilitates the next step for extracting the boundary.

According to Susan standards on edge detection, the four key components' outline sizes of the axial projection planes are ultimately obtained; through the image digitization, useful data is extracted and the outline size is converted to the same coordinates, and then the data is recorded in the coordinates form to facilitate further calculations.

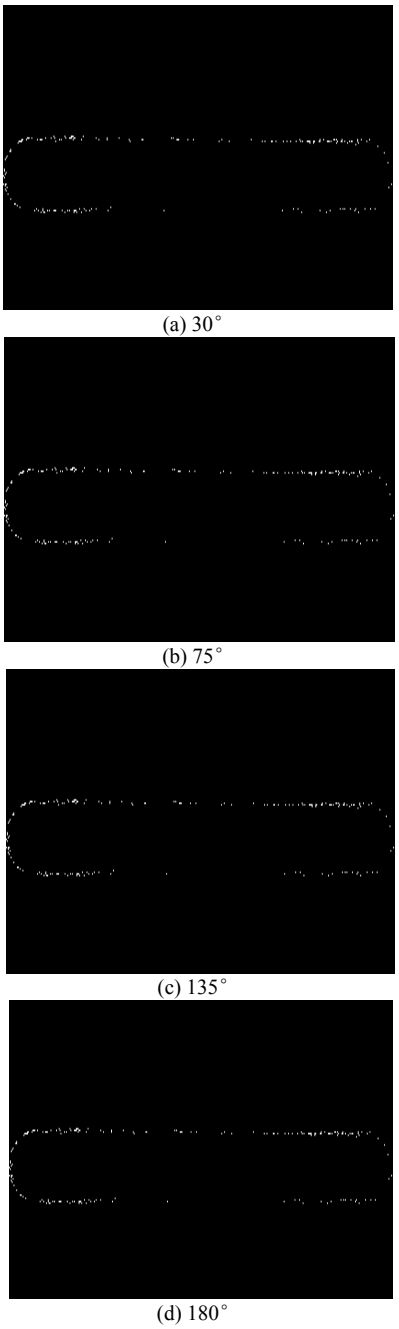

(a) 30°

(b) 75°

(c) 135°

(d) 180°

Figure 5. Four axial projection plane information.

C. Error Evaluation

After image analysis, we can get the required data which are mainly outline information; however other information related to the parts can be derived indirectly from the formula. In the learning process of precision instruments, we found that the coordinate measuring machine took four or eight points of the measured body

to analyze; the data collection mode is similar with this paper. Therefore, the information obtained from image analysis is compared with the information obtained from coordinate measuring machine, as shown in Table 2 to Table 5.

TABLE II.
COMPARISON OF TWO DATA PROCESSING (1)

Comparison type	Test group number	Image processing measurement results	Coordinate measuring machine results
Minimum radius of concentric circles (mm)	1	24.8432	24.8436
	2	24.8520	24.8516
	3	24.7231	24.7237
	4	24.8438	24.8434
	5	24.8515	24.8514
	6	24.7233	24.7235

TABLE III.
COMPARISON OF TWO DATA PROCESSING (2)

Comparison type	Test group number	Image processing measurement results	Coordinate measuring machine results
Maximum radius of concentric circles (mm)	1	25.6989	25.6992
	2	25.5202	25.5205
	3	25.7035	25.7033
	4	25.6995	25.6992
	5	25.5217	25.5214
	6	25.7023	25.7026

TABLE IV.
COMPARISON OF TWO DATA PROCESSING (3)

Comparison type	Test group number	Image processing measurement results	Coordinate measuring machine results
Roundness error (mm)	1	0.8597	0.8594
	2	0.8475	0.8472
	3	0.7980	0.7980
	4	0.8587	0.8585
	5	0.8462	0.8459
	6	0.8054	0.8043

TABLE V.
COMPARISON OF THE TWO DATA PROCESSING (4)

Comparison type	Test group number	Image processing measurement results	Coordinate measuring machine results
Cylindricity error (mm)	1	0.0214	0.0208
	2	0.0197	0.0197
	3	0.0221	0.0213
	4	0.0199	0.0198
	5	0.0216	0.0209
	6	0.0209	0.0207

VI. CONCLUSIONS

According to the testing precision, visual inspection is applied to the geometry detection of key parts, which simplifies the work platform and improves the geometric detection efficiency meanwhile.

The mechanical splicing solutions using a CCD device can solve the geometry detection problem of large-size key components. Besides, the visual detection can be applied to large-size objects from small–size objects.

By comparison of several image-processing programs, a more reasonable image processing program is put forward. It provides sufficient data information for the detection of the key components' size and shape error and lays the foundation for the geometric quantity intelligent detection of coal mining machinery.

ACKNOWLEDGMENT

Financials support for this work, provided by the Jiangsu Graduate education innovation Project fund (Project No. CXZZ12_0929) and the Priority Academic Program Development of Jiangsu Higher Education Institution, are gratefully acknowledged.

REFERENCES

[1] J. G. Wu, H. Z. Bin, "The thin part size machine vision inspection system", *Optics and Precision Engineering*, vol. 15, no. 1, pp. 124-130, 2007.
[2] D. Williams, P. D. Burns, "Low-frequency MTF estimation for digital imaging devices using slanted edge analysis", *Proc. SPIE-IS&T Electronic Imaging Symposium*, vol. 5294, no. 1, pp. 93-101, 2004.
[3] B. Skarman, J. Becker, K. Wozniak, "Simultaneous 3D-PIV and temperature measurements using a new CCD-based holographic interferometer", *Flow Measurement and Instrumentation*, vol. 33, no. 10, pp. 1711-1716, 2004.
[4] P. F. Luo, "Application of computer vision and laser interferometer to the inspection of line scale", *Optics and Lasers in Engineerin*g, vol. 5, no. 42, pp. 563- 584, 2004.
[5] C. J. Tay, S. H. Wang, C. Quan, "Measurement of a micro-sol-derball height using a laser projection method", *Optics Communications*, vol. 234, no. 1-6, pp. 77-86, 2004.
[6] G. Sutter, L. Faure, A. Molinari, "An experimental technique for the measurement of temperature fields for the orthogonal cutting in high speed machining", *International Journal of Machine Tools and Manufacture*, vol. 43, no. 7, pp. 671-678, 2003.
[7] F. Wan, S. F. Fan, "C8051F020 is the core of CCD driver and Acquisition System design", *Optics and Precision Engineering*, vol. 13, pp. 179-182, 2005.
[8] Y. Liu, C. C. Zuo, Y. M. Zhang, "Large cylindrical work piece shape and position error detection method", J*ournal of Liaoning Technical University*, vol. 26, no. 3, pp. 428-431, 2007.
[9] C. X. Sheng, T. Zhang, J. Jing, "High-resolution CCD chip FTF4052M drive system design", *Optics and Precision Engineerin*g, vol. 15, no. 4, pp. 564-569, 2007.
[10] Y. F. Qu, Z. B. Pu, Y. A. Wang, "Visual inspection system in Central Asia-pixel edge detection technique comparative study", *Journal of Scientific Instrument*, vol. 24, no. 4, pp. 460-462, 2003.
[11] S. Hartmann, T. Tschöpe, L. Schreiber, P. Haupt, "Finite deformations of a carbon black-filled rubber, Experiment, optical measurement and material parameter identification using finite elements", *European Journal of Mechanics-A/Solid*s, vol. 22, no. 3, pp. 309-324, 2003.
[12] O. Alaa, O. Frederik, A. Marcus, "Temperature measurements of combustible and non-combustible surfaces using laser induced phosphorescence",

Experimental Thermal and Fluid Science, vol. 28, no. 7, pp. 669-676, 2004.
[13] X. J. Wu, D. Zhang, "Roundness error processing based on Particle swarm optimization", *Journal of Sensor Technology*, vol. 28, no. 7, pp. 669-676, 2007.
[14] M. Clerc, J. Kennedy, "The particle swarm explosion, stability, and convergence in a multidimensional complex space", *IEEE Transactions on Evolutionary Computation*, vol. 6, no. 1, pp. 58-73, 2002.
[15] C. C. Cui, F. G. Huang, R. C. Zhang, B. Li, "Research on cylindricity evaluation based on the Particle Swarm Optimization", *Optics and Precision Engineerin*g, vol. 14, no. 2, pp. 256-260, 2006.

Chenxu Luo , Male,Born in 1986, Doctoral candidate of China University of Mining and Technology, China.

Changlong Du ,Male,Born in 1958, a professor of China University of Mining and Technology, China.

Wan Ma,female, Born in 1988, Doctoral candidate of China University of Mining and Technology, China.

[16] C. C. Cui, F. G. Huang, R. C. Zhang, B. Li, "Roundness Error Evaluation Based on the Particle Swarm Optimization", *ACTA METROLOGICA SINICA*, vol. 27, no. 4, pp. 317-320, 2006.
[17] X. D. Shen, J. Y. Liu, Y. Liu, "Pheromone-sharing mechanism Particle Swarm Optimization for restoring solutions in electric power systems", *International Journal of Advancements in Computing Technology*, vol. 4, no. 7, pp. 291-298, 2012.